33rd Annual International Conference of the IEEE EMBS
Boston, Massachusetts USA, August 30 - September 3, 2011

Electrical Impedance Tomography Reconstruction Through Simulated Annealing with Incomplete Evaluation of the Objective Function

Thiago de Castro Martins and Erick Dario León Bueno de Camargo
Raul Gonzalez Lima and Marcelo Brito Passos Amato
Marcos de Sales Guerra Tsuzuki

Abstract— **The EIT reconstruction problem is approached as an optimization problem where the difference between a simulated impedance domain and the observed one is minimized. This optimization problem is often solved by Simulated Annealing (SA), but at a large computational cost due to the expensive evaluation process of the objective function. We propose here, a variation of SA applied to EIT where the objective function is evaluated only partially, while ensuring upper boundaries on the deviation on the behavior of the modified SA. The reconstruction method is evaluated with simulated and experimental data.**

I. Introduction

EIT is an imaging modality that estimates the electrical conductivity distribution within the body when a low amplitude current pattern is applied to its surface and the potential at determined points of that surface is measured through electrodes or, alternatively, when a potential is applied and the current flowing through the surface is measured [1]. The two main forms of EIT are dynamic imaging and static imaging yielding differential and absolute images respectively. The images produced by differential imaging represent the conductivity changes of a region between two time intervals [2]. Imaging physiological function within the body largely relies on this technique. This work, is mainly concerned with the reconstruction of static conductivity images which requires more advanced numerical algorithms.

This paper is structured as follows. Section II presents the problem formulation where it is explained how the EIT reconstruction problem can be approached as an optimization problem. Section III explains the proposed algorithm where a SA with incomplete evaluation of the objective function is used to solve the EIT reconstruction problem. In section IV some results obtained from physical data are presented. Finally, section V rounds up the paper with the conclusions.

II. Formulation

The typical forward problem in EIT is given the conductivity distribution σ and the current J injected through boundary electrodes, find the potential distribution ϕ within Ω and in particular the resulting potentials at the measurement electrodes ϕ_m. The frequencies used in EIT are low enough so that the quasi-static approximation hold, and thus we can ignore capacitive and inductive effects. Under such quasi-static conditions, the solution of the forward problem is rather simple as it only requires solving the Laplace equation

$$\nabla(\sigma\nabla\phi) = 0 \tag{1}$$

At the boundary, currents are injected through electrodes; thus the current density through the l-th electrode surface J_l is given by

$$\sigma\frac{\partial\phi}{\partial\hat{n}} = J_l \tag{2}$$

where $\hat{n}$ is the external normal versor and zero elsewhere at the boundary. Data is collected by injecting current with a single source and measuring voltage. There are several ways in which the pair of electrodes is switched and the voltage measurements are collected in the literature [3].

A. Finite Element Model

The inverse problem is formulated as given the injected currents J and the potentials at measurement electrodes ϕ_m, find the electrical conductivity distribution σ within Ω. In practice only a finite number of potential measurements is made through the electrodes, so the Dirichlet boundary condition is incomplete [4]. For an irregular domain and isotropic media, analytical solution to the Laplace equation (1) with boundary condition (2) are unknown; thus, the partial differential equations were approximated by the finite element method (FEM), the domain is discretized with triangular linear elements with constant conductivity and both problems, forward and inverse, are solved numerically. The virtual potential principle associated with the Laplace equation provides the local element matrices.

When the local element matrices are stated in terms of the global coordinates of the mesh, the global conductivity matrix [1] which includes electrode contact impedance effects, is obtained; then the following relation holds

$$\boldsymbol{K}\cdot\boldsymbol{\Phi} = \boldsymbol{C} \tag{3}$$

where $\boldsymbol{K}(\sigma) \in \Re^{s\times s}$ is the conductivity matrix calculated at a given particular distribution σ, $\boldsymbol{\Phi}$ is a matrix containing nodal potentials corresponding to each applied current

This work was supported by FAPESP (Grants 2009/07173–2 and 2010/19380–0). TC Martins was supported by FAPESP (Grant 2009/14699–0). MSG Tsuzuki was partially supported by CNPq (Grants 304.258/2007–5 and 309.570/2010–7). TC Martins and MSG Tsuzuki are with Computational Geometry Laboratory, Escola Politécnica, São Paulo University, Brazil. thiago@usp.br. RG Lima and EDLB Camargo are with Department of Mechanical Engineering, Escola Politécnica, São Paulo University, Brazil. MBP Amato is with Respiratory Intensive Care Unit, Pulmonary Division, Hospital das Clínicas, University of São Paulo, Brazil.

pattern, and $\boldsymbol{C}$ represents p linearly independent current patterns.

B. The Inverse Problem as an Optimization Problem

Since there are known methods for efficiently solve the forward problem (such as FEM), one possible approach to the inverse problem is to look at it as an optimization problem, where the optimization variables are a parametrization of the conductivity inside the domain and the optimization function is some measure of how the solution of the forward problem applied to the conductivity distribution produced by the optimization variables matches the measured data. One possible objective function $E(\sigma)$ is the Euclidean distance between the measured electric potentials ϕ_m^i and the calculated potentials $\phi_c^i(\sigma)$ for the i-th applied current pattern:

$$E(\sigma) = \sqrt{\Sigma|\phi_m^i - \phi_c^i(\sigma)|_2} \tag{4}$$

Mello et al. [5] proposed an example of such approach, where the objective function (4) is minimized by Sequential Linear Programming yielding estimations of the conductivity distribution. It was also pointed that it is difficult to solve this problem by methods based on gradients of the objective function due to the fact that the problem is often ill-posed. Numerical errors in the calculation of the objective function are greatly amplified in its derivatives. That is why the interest on SA applied to EIT is increasing, as it requires no evaluation of objective function derivatives (in fact, as we will show, it does not even require a complete computation of the objective function).

III. Applying Simulated Annealing to EIT

Herrera et al. [6] minimized objective function (4) with SA and by doing so, managed to reconstruct very accurate conductivity distributions of the body, but at a very high computational cost. This is unsurprising, as each step of the SA involves the solution of a full FEM problem in order to evaluate the objective function.

A. Incomplete Evaluation of the Objective Function

As the evaluation of the objective function is responsible for the bulk of the SA, it is interesting to look for means to reduce its cost. An example of SA with incomplete evaluation of the objective function can be seen in [7], where an estimate of the probability distribution of the objective function is used instead of the actual value. In this work, it is presumed that the exact distribution of the objective function is unknown, and it is proposed an iterative computation process that yields boundaries for its values. There is a relationship between those boundaries and the probability of deviation of the algorithm from an exact SA. Using those relationships and imposing upper limits for those probabilities, stopping criteria for the interactive calculation of the objective function are obtained. The objective function is given by (4). The calculated potentials ϕ_c^i for each current pattern are obtained from a FEM algorithm whose kernel is a solver for the linear system posed by (3).

The Conjugate Gradient (CG) method is usually used to solve such linear systems [8] as matrix $\boldsymbol{K}$ is sparse, symmetric and positive–definite. Meurant [9] proposed a method to estimate an upper bound for the l_2 norm of the error of the CG method at each iteration. Such bound can be used to estimate a bound on the error of the objective function (4) when the exact FEM solutions ϕ_c are replaced by partial solutions $\tilde{\phi}_c$ obtained by stopping the CG method before the final convergence. This is done by taking the conservative assumption that all the error is concentrated on the electrode nodes. Then, if $d^i = \left|\phi_m^i - \phi_c^i\right|$ is the component of the objective function for a given current pattern, $\tilde{d^i} = \left|\phi_m^i - \tilde{\phi}_c^i\right|$ is its estimate obtained with the partial solution $\tilde{\phi}_c$ and $\varepsilon^i \geq \left|\phi_c^i - \tilde{\phi}_c^i\right|$ is an upper boundary on the error of the CG method, we have

$$\begin{aligned} \tilde{E} &= \sqrt{\Sigma\left(\tilde{d^i}\right)^2} \\ E \leq E_{max} &= \sqrt{\Sigma(d^i + \varepsilon^i)^2} \\ E \geq E_{min} &= \sqrt{\Sigma \max\{d^i - \varepsilon^i, 0\}^2} \end{aligned} \tag{5}$$

The upper and lower boundaries for E converge to the exact value as the number of multiple CG iterations increase. As SA is sensible only to relative variations of the objective function those boundaries must be converted to variation of E boundaries. If $\Delta E = E^j - E^{j+1}$ is the variation of the objective function when the SA process moves from one solution x^j to another x^{j+1} then, by interval arithmetics,

$$\begin{aligned} \Delta\tilde{E} &= \tilde{E}^j - \tilde{E}^{j+1} \\ \Delta E \leq \Delta E_{max} &= E_{max}^j - E_{min}^{j+1} \\ \Delta E \geq \Delta E_{min} &= E_{min}^j - E_{max}^{j+1} \end{aligned} \tag{6}$$

Again, those boundaries for ΔE converge to the exact value, but this time, it is necessary to increase the number of iterations for both evaluations: x^j and x^{j+1}.

From that, it can be seen that a SA process that would use the partial FEM solutions $\tilde{\phi}_c$ instead of the exact ones ϕ_c would have a limited probability of diverging from the process that uses the exact solutions. Indeed, by imposing P_{err} as an upper limit on the probability of the process taking a "wrong" decision (rejecting a solution when it should accept it or accepting when it should reject), conditions for the boundaries in (6) are defined:

$$e^{-\Delta E_{max}/kt} \geq \begin{cases} 1 - P_{err} & \text{if } \Delta\tilde{E} \leq 0, \\ e^{-\Delta\tilde{E}/kt} - P_{err} & \text{if } \Delta\tilde{E} > 0 \end{cases} \tag{7}$$

$$e^{-\Delta E_{min}/kt} \leq min(1, P_{err} + e^{-\Delta\tilde{E}/kt}) \tag{8}$$

These conditions do not translate directly into stopping criteria for the CG algorithm, as ΔE_{max} and ΔE_{min} are the partial solutions of two separated sets of FEM problems, and in general, they are not reachable by tightening the boundaries in just one set. As such, every solution must have its objective function evaluation process stored so it may be possible to continue it from where it has stopped.

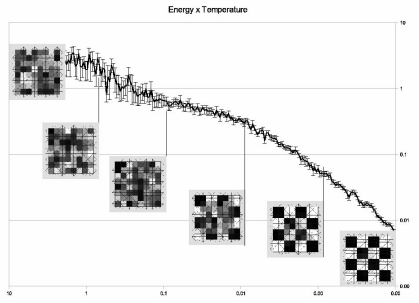

Fig. 1. Energy (Objective Function) $\times$ Temperature graph for the "checkerboard" problem (error bars represent the standard deviation at a fixed temperature).

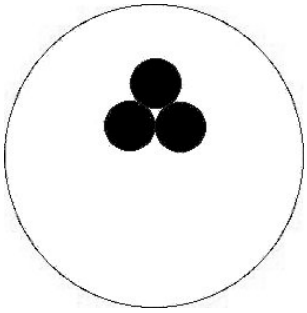

Fig. 2. Layout of the experiment. Small circles represent cucumber slices immersed in the salt solution.

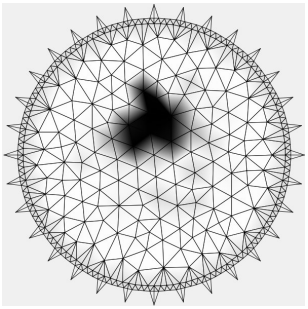

Fig. 3. Reconstructed image from experimental data.

IV. Results

To evaluate the viability of SA with partial evaluation applied to the EIT problem, a simple implementation was built using a simulated domain: a square, measuring 16×16 units, composed of 76 triangular elements with 320 nodes, of whose 32 are electrodes. The electric conductance domain was divided in 64 2×2 squares (notice the potential discretization and the conductance discretization are not the same). The FEM problems were solved using a CG method with Incomplete Choleski decomposition preconditioning [10]. The 64 conductivity parameters are generated by SA. The neighborhood heuristic used by the SA was taken from [11], changing only a single conductivity parameter at each iteration and reducing the modifications on parameters that lead to rejected solutions. The divergence probability P_{err} was arbitrarily defined as $1/100$. The simulated problem is a 4×4 "checkerboard" conductivity pattern, alternating high conductivity (2) and low conductivity (1). The SA process has accurately reconstructed the conductivity distribution. The examination of intermediary results, displayed on Fig. 1 shows that the impedance distribution is reconstructed from the outside towards the interior of the domain.

The evaluation of a method for reverse problems with synthetic data, (particularly when a single model is used both for the production of data and its inversion) can be misleading [12]. Indeed, the graph in Fig. 1 shows that, as the temperature decreases, the difference between the electrode potentials of the original model and the reconstructed one tends to zero. While expected, this behavior is unrealistic, as in practical applications, the simulated model will always differ from the physical system. It is thus necessary to evaluate the proposed reconstruction process when applied to data obtained from a physical system.

For that, a simple model was built, composed of a cylindric container made of acrylic measuring $300mm$ in diameter, with 32 electrodes equally spaced in the outer wall. The electrodes are prismatic, that is, their cross-sections are invariant. The container was filled with saline water up to a height of $25mm$. The current was applied to the model in "jump-three" patterns, that is, the current was applied between two electrodes that were four positions apart (that is, separated by three electrodes). Those patterns were applied to each of the 32 electrodes. The applied current was of about $10mA$ (actual values varied at each application) AC at $125Hz$. In order to produce observable phantoms, three slices of cucumber (see [13] for a study of cucumber as a material for EIT evaluation), slightly thicker than the solution height (but not enough to produce significant 3D effects) where inserted in a triangular pattern as seen in Fig. 2. Data was collected for both the empty saline solution and for the solution with cucumber slices.

For the simulated model, a FEM model was created with 750 triangular elements and 450 nodes. Observing the data collected with the empty medium, it became obvious that the impedance of each electrode varies significantly. In a first step, to precisely obtain the impedance for each electrode, the reconstruction process was executed with the

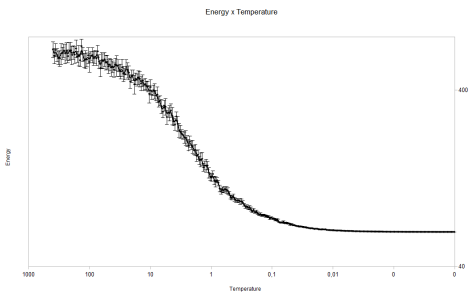

Fig. 4. Energy (Objective Function) $\times$ Temperature graph for the reconstruction from experimental data (error bars represent the standard deviation at a fixed temperature).

empty medium data, presuming uniform (but unknown) conductivity inside the simulated model and independent conductivity impedance values for each electrode (yielding an optimization problem of $32+1$ unknowns). To reconstruct the cucumber phantoms, the conductivity distribution in the simulated model was parameterized using the same 1st-order interpolating functions used for the potential in the FEM (the parameters being the conductance value at each node). The conductance of the electrodes was fixed at the values obtained in the first step, and so was the conductance for the "outer ring" elements.

The reconstructed phantom can be seen in Fig. 3. As one can see, despite being heavily constrained by the mesh coarse discretisation, the reconstructed conductance distribution is a reasonable image of the physical phantom, evoking a vaguely triangular shape. The qualitative convergence can be seen in Fig. 4. Comparing with data in Fig. 1, it is clear that the energy no longer decreases freely, hitting instead an "error floor" induced by the FEM errors. The final reconstruction error is of about 62V. This accounts for the total difference on all 32 electrodes and all 32 current patterns between observed data and the simulation results. Taking into account the normalization of the observed potentials and considering an uniform distribution of errors, this represents an error of less than 2% per electrode at each observed current pattern. The impact of partial evaluation objective function in the process performance can be seen in Fig. 5, showing the average number of CG iterations used by the process at each temperature. Considering that the system has over 450 nodes, it is remarkable that the system is able to achieve those results while using in average less than 30 iterations of CG. More interesting is the evolution of the iteration number as the optimization progresses. At high temperatures, the high kt and $\Delta\tilde{E}$ values lead to relatively loose conditions in (7) and (8), reachable by few iterations of the CG algorithm. As the temperature diminishes, lower kt and $\Delta\tilde{E}$ values impose through (7) and (8) tighter conditions, leading to a higher number of CG iterations. It may be a bit surprising that as the process converges towards the final solution, the number of CG iterations reduces again. This is explained by two factors. First, the "initial guess" for the CG algorithm is obtained from the solution obtained at the previous solution of the SA algorithm. Second, the adaptive neighborhood heuristic reduces dramatically the modifications on the conductivity distribution as the process converges towards a global optimum [11]. Combining those two factors, it can be seen that in the final convergence of the optimization process, the previous FEM solutions are an initial guess good enough to compensate for the increasingly severer conditions on the boundaries of ΔE. The process showed in Figs. 4-5 has deliberately extreme annealing parameters, with a too high initial temperature and too low final temperature. The whole process took over 8 hours to complete. The image in Fig. 3 was reconstructed using an initial temperature of just 0.05 and final temperature of 0.0075 and was completed under 55 minutes on an intel i7 3.2 GHz CPU. It is worth of notice that the code is yet unoptimized, using a single thread of execution and 32 bits architecture.

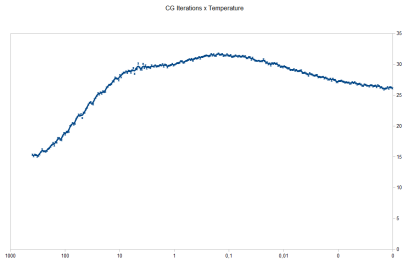

Fig. 5. CG Iterations $\times$ Temperature for the reconstruction from experimental data.

V. Conclusions

It is proposed a new approach to solve the EIT inverse problem using a SA with incomplete evaluation of the objective function. It is showed, in the particular case of EIT, how it is possible to enforce upper bounds on the probability of the modified SA by converting those bounds in stopping criteria for the inner CG algorithms used to solve the forward EIT problem. Initial results, both with synthetic and experimental data, show that while the partial evaluation of objective functions does not compromise the convergence of the SA algorithm, it has a great potential of improving its efficiency.

References

[1] FC Trigo, RGLima, and MBP Amato, "Electrical impedance tomography using the extended kalman filter," *IEEE T Biomed Eng*, vol. 51, pp. 72–81, 2004.

[2] DC Barber and BH Brown, "Applied potencial tomography," *J Phys E Sci Instrum*, vol. 17, pp. 723–733, 1984.

[3] BH Brown and A Seagar, "The sheffield data collection system," *Clin Phys Physiol Meas*, vol. 8, pp. A91–A97, 1987.

[4] FS Moura, KCC Aya, AT Fleury, MBP Amato, and RG Lima, "Dynamic imaging in electrical impedance tomography of the human chest with online transition matrix identification," *IEEE T Biomed Eng*, vol. 57, pp. 422–431, 2010.

[5] LAM Mello, CR Lima, MBP Amato, RG Lima, and ECN Silva, "Three-dimensional electrical impedance tomography: a topology optimization approach." *IEEE T Biomed Eng*, vol. 55, no. 2 Pt 1, pp. 531–40, 2008.

[6] CNL Herrera, MFM Vallejo, FS Moura, JCC Aya, and RG Lima, "Electrical impedance tomography algorithm using simulated annealing search method," in *Proc COBEM*. Brasília: ABCM, 2007.

[7] S Lakshmanan and H Derin, "Simultaneous parameter estimation and segmentation of gibbs random fields using simulated annealing," *IEEE T Pattern Anal Mach Intell*, vol. 11, pp. 799–813, 1989.

[8] JR Shewchuk, "An introduction to the conjugate gradient method without the agonizing pain," Carnegie Mellon University, Pittsburgh, PA, USA, Tech. Rep., 1994.

[9] G Meurant, "Estimates of the l2 norm of the error in the conjugate gradient algorithm," *Numerical Algorithms*, vol. 40, no. 2, pp. 157–169, Oct. 2005.

[10] S Kershaw, "The incomplete Cholesky-Conjugate Solution of Systems," *J Comput Phys*, vol. 65, pp. 43–65, 1978.

[11] TC Martins and MSG Tsuzuki, "Placement over containers with fixed dimensions solved with adaptive neighborhood simulated annealing," *B Pol Acad Sci Techn Sci*, vol. 57, pp. 273–280, 2009.

[12] A Wirgin, "The inverse crime," *ArXiv Math Phys e-prints*, Jan. 2004.

[13] DS Holder, Y Hanquan, and A Rao, "Some practical biological phantoms for calibrating multifrequency electrical impedance tomography," *Physiol Meas*, vol. 17, no. 4A, p. A167, 1996.